Supplementary Information for

CaSiAn: Calcium Signal Analysis Software

Ca^{2+} signals are typically determined by averaging or getting the mean pixel intensities in the regions of interest from a time series of fluorescence images. Hence, each signal is a discrete-time function that can be represented as a set of paired values $sg = \{(t_k, f_k), k = 1,..,N\}$ where f is the intensity at time point t, k is the frame number and N is the total number of successive Ca^{2+} images. In the CaSiAn data structure, each signal is therefore a discrete-time function that can be represented as a set of paired values of the intensity and the corresponding time point.

In this supplementary material, we give first an illustrative summary of the CaSiAn workflow and subsequently describe the methods for removing signal background by baseline estimation and the signal normalization. Then, we explain in detail the constraint-based algorithms that CaSiAn implements for finding peaks and nadirs of Ca^{2+} signals and false positive filtering. Next, we describe how signal features are determined by the CaSiAn algorithms. We then give a tool overview and outline step by step how to set up a CaSiAn analysis. Finally, we give the experimental details of the performed experiments.

Contents

Contents **1**

S1 Illustrative Summary of the CaSiAn workflow . . . 2
S2 Background Removal and Normalization . . . 2
S3 Peak and Nadir Detection . . . 5
S4 Feature Extraction . . . 6
S5 Quick guide . . . 13
S5.1 Setup . . . 13
S5.2 Preprocessing . . . 14
S5.3 Feature Extraction . . . 14
S6 Materials and Methods . . . 15
S6.1 Ca^{2+} Imaging in C8-D1A cells . . . 15
S6.2 Zebrafish Calcium Imaging . . . 16

Bibliography **21**

S1 Illustrative Summary of the CaSiAn workflow

A typical workflow of the CaSiAn based analysis is shown in Fig. S1 for the astrocytes experiments described in the main text and detailed below in Section S6.1. Based on extracted signals, CaSiAn enables background removal and normalisation, determination of ISIs, spike characterization and investigation of the linear σ – T_{av} relation. Finally, all data can be exported for further analysis.

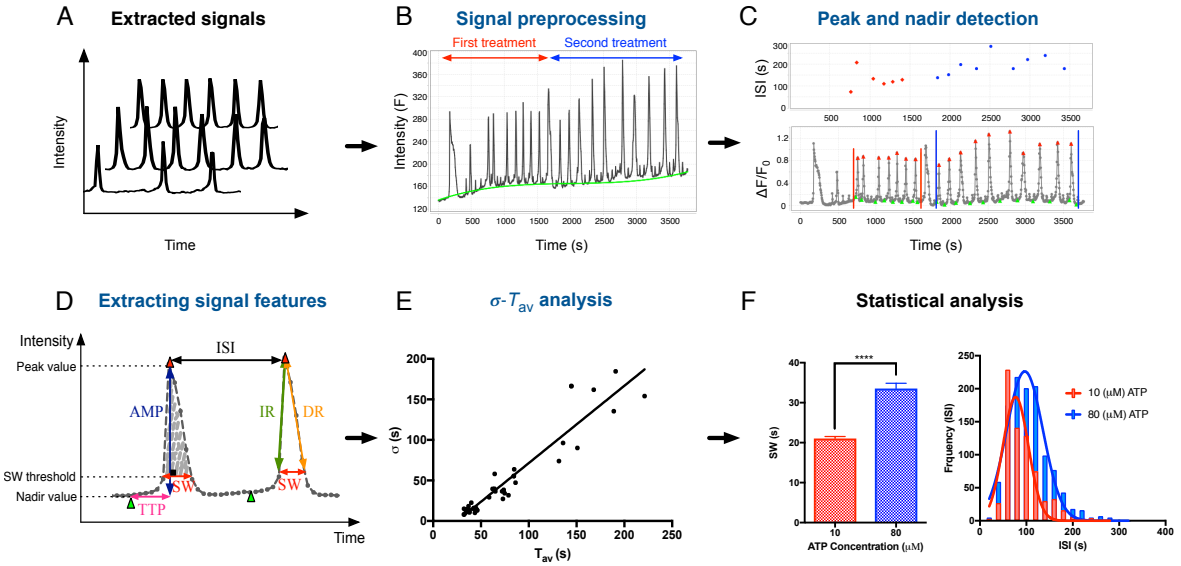

Figure S1. Workflow of CaSiAn. (A) Time course data extracted from fluorescence images are loaded into CaSiAn. (B) Preprocessing allows for defining different analysis periods (red and blue, respectively), normalization and background removal by several non-linear fitting methods. (C) Peaks and nadirs are automatically detected by threshold parameters interactively adjustable in the GUI. Misclassified peaks and nadirs can be interactively added or removed leading to identification of individual ISIs. Note that in the case of stimulation, cells typically exhibit an initial transient phase which should be excluded for spiking analysis as indicated by the horizontal bars in the lower panel. (D) Based on the processed time courses, CaSiAn determines signal properties like ISI, amplitude, spike width and further characteristics. (E) After automated processing of all signals, CaSiAn offers to plot the σ – T_{av} relation where each dot corresponds to an individual signal. This relation can be further analyzed in an interactive manner. (F) Finally, all processed signals including ISI detection can be saved in a single pdf file and determined signal characteristics can be exported as csv or excel files for further analysis.

S2 Background Removal and Normalization

CaSiAn can represent the intensities of Ca^{2+} signals in two common ways: (1) by the ratio of the relative fluorescence change and the baseline fluorescence (I) and (2) by the ratio of fluorescence intensity and the baseline fluorescence (I').

$$I(k) = \frac{f(k) - F_0(k)}{F_0(k)}, \tag{S1}$$

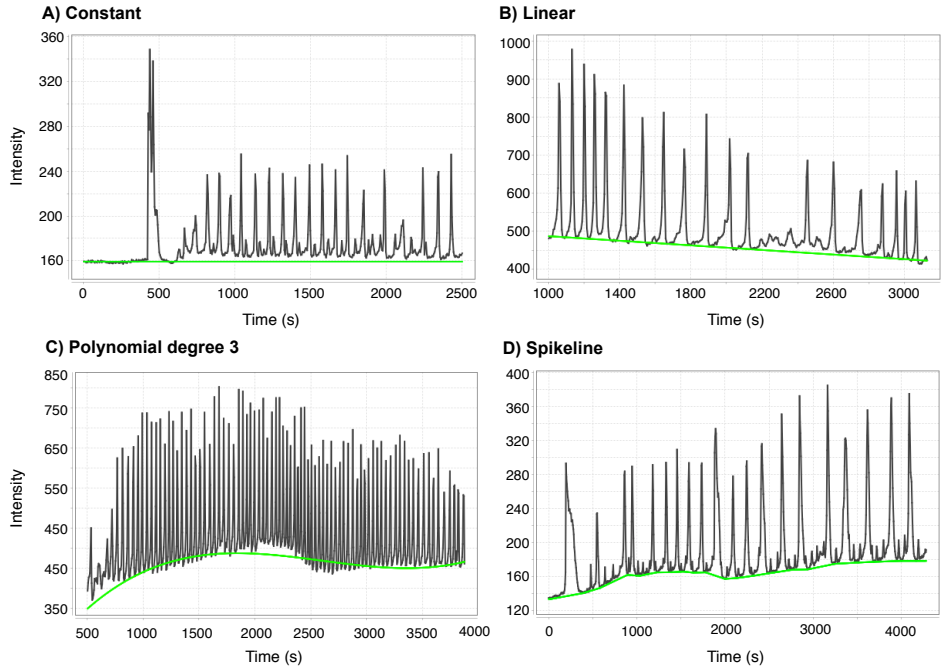

Figure S2. CaSiAn can fit different curves to the signal baseline. The user is able to select a curve type from a list and CaSiAn determines the best fitting-curve to the signal baseline (green). Then the estimated baseline can be removed from the signal and subsequentlly the signal can be normalized.

$$I'(k) = \frac{f(k)}{F_0(k)}, \tag{S2}$$

where $f(k)$ is the intensity of a region of interest at frame k and $F_0(k)$ is the background intensity at frame k [Waters, 2009]. Function I subtracts the background intensities from the signal intensities and then normalize the results by dividing them to the background intensities. Since finding the real background function F_0 is not a trivial task, CaSiAn has implemented the following different inference methods for background florescence $\hat{F_0}$ summarized in Fig. S2:

Constant Baseline. One simple way for estimating the baseline is considering constant background. In this method, $\hat{F_0}$ is determined by averaging signal intensities during the resting state of the cell:

$$\hat{F_0} = \frac{1}{n}\sum_{k=1}^{n} f(k), \tag{S3}$$

where k is the index of image frame and n is the frame number of the first peak in the signal.

Curve Fitting. The curve fitting method provides more precise approximation of the signal background since it considers fluorophore leaking and photobleaching, i.e. fading the emitted fluorescence during observation [Diaspro *et al.*, 2006]. In the curve fitting method,

CaSiAn removes the trends of the signal baseline by fitting a curve to the data set $po_{min} = \{(t_{m_k}, f_{m_k}), k = 1, .., n\}$ $(t_{m_k} < t_{m_{k+1}})$, where f_m is the minimum intensity in the area between two consecutive peaks, t_m is the time of the minimal intensity and n is the number of ISIs [Mikhailyuk and Razzhivin, 2003, Balkenius *et al.*, 2015]. CaSiAn implements the following curve fitting techniques for estimating the $\hat{F}_0$ function:

Linear Regression (LR). Regression techniques are able to estimate the parameters of a best-fit curve to the signal baseline by minimizing the sum squared error of the signal baseline and estimated curve. Linear regression infers the signal baseline $\hat{F}_0$ then as a linear function:

$$\hat{F}_0(t, f) = \beta_0 + \beta_1 t \ . \tag{S4}$$

Polynomial Regression (PR). Polynomial regression assumes that F_0 is a nonlinear function. The inferred function $\hat{F}_0$ takes the form of an mth-degree polynomial:

$$\hat{F}_0(t, f) = \beta_0 + \sum_{i=1}^{m} \beta_i t^i \ . \tag{S5}$$

CaSiAn implements PR($m = 2$, 3, 4) because based on our experiments they can predict the background curve of the majority of signals while by increasing m the goodness of the fit decreases. The parameters β_i have to be estimated using the po_{min} data set.

Spike Base Line. This method infers one $\hat{F}_0$ for each spike using the line that connects two consecutive points of the po_{min} data set. Let (t_{m_k}, f_{m_k}) and $(t_{m_{k+1}}, f_{m_{k+1}})$ be two consecutive points in the po_{min} data set, $\hat{F}_{0k}$ is inferred as:

$$\hat{F}_{0k}(t, f) = \beta_{0k} + \beta_{1k} t \tag{S6}$$

where the slope of $\hat{F}_{0k}$ is:

$$\beta_{1k} = (f_{m_{k+1}} - f_{m_k}) / (t_{m_{k+1}} - t_{m_k}) \tag{S7}$$

Background correction by the curve fitting method leads to zero for the minimal signal intensity. In some signals, subtracting estimated background from the signal intensities may cause negative values. In this case, CaSiAn computes the minimum of all negative values and offsets all signal intensities by the absolute value of this minimum that finally result in a zero value for the minimal signal intensity.

We also implemented a version of CaSiAn that allows background removal for the two fluorescent channels of a ratiometric fluorescent dye independently. This version is also available from the download section of the project webpage (http://r3lab.uni.lu/web/casa/)

S3 Peak and Nadir Detection

The existing noise in the florescence Ca^{2+} images renders the peak detection process difficult. Although applying smoothing techniques like signal or image filtering may increase signal to noise ratio, it may substantially change the shape and features of Ca^{2+} spikes [Balkenius *et al.*, 2015, Janicek *et al.*, 2013] which can distort the experimental results. A common practice for enhancing the performance of peak detection algorithms in noisy data is defining a sliding window with the length of the signal periodicity and identifying global maximum values within the window as signal peaks. But this technique is not applicable to Ca^{2+} signals since they are often non-periodic signals with interspike intervals of different lengths.

In the CaSiAn tool, we have introduced a new constraint-based method for finding peaks and nadirs of Ca^{2+} signals that only needs one parameter set by the user. This algorithm contains the following steps:

1. Finding the local maxima (local peaks) and local minima (local nadirs) in the signal.
2. Identifying the initial list of global peaks by selecting local peaks that have a mean edge magnitude higher than the peak threshold parameter. The magnitude of a peak edge is defined as the intensity difference between peak value and its prior and succesive nadir. The peak threshold parameter is defined by the user as the percentage of the maximum amplitude that occurs in the signal where the maximum amplitude in a signal is the maximal intensity difference between two consecutive local nadir and local peak. In summary, the two edges of each local peak are averaged and then the peaks with a mean peak edge magnitude higher than the amplitude threshold are selected as the initial list of global peaks.
3. Finding the final list of signal peaks by filtering the initial list of global peaks. If two consecutive local peaks specified in step 1 are also identified as two global peaks in step 2, then one of these two peaks might be false positive (see Fig. S3, A′, B′, D′, E′). Detecting two consecutive local peaks as two global peaks of the signal is not expected and typically correspond to noise between global peaks. In order to decide on the detection correctness, another constraint is applied to these peaks based on the expected shape of a peak. This constraint checks whether the height of the shorter edge of the peak is more than fifty percent of the longer edge height. If even one of the peaks does not meet this condition (see Fig. S3, B′ and D′), then only one peak should be selected as global peak which is the one with the higher intensity (see Fig. S3, A′ and E′).
4. Identifying the corresponding nadir for each peak. Let $t_p = (t_{p_1}, t_{p_2}, ..., t_{p_n})$, $t_{p_k} < t_{p_{k+1}}$ be the vector of peak times, where n is the total number of detected peaks. The nadir of

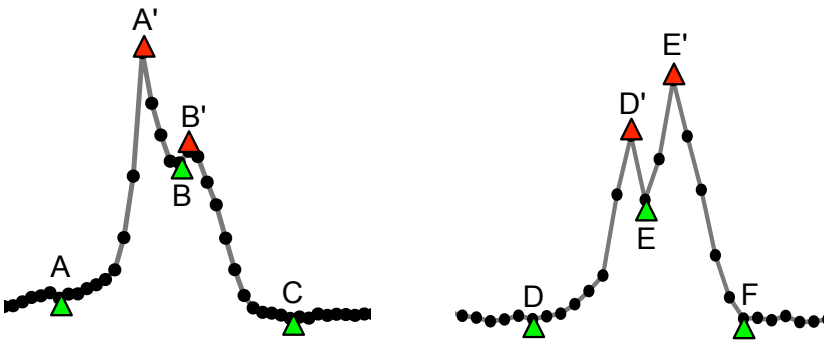

Figure S3. Detecting and removing false positive peaks. In step (2) of the peak detection algorithm, points A′, B′, D′, E′ are detected as potential signal peaks. In step (3) of the algorithm, points B′, D′ are identified as false positives and only points A′ and E′ are detected as signal peaks. Points A, B, C, D, E and F are local minima. In step (4) of the algorithm, points A and D are identified as nadirs.

k-th peak is identified as the minimum intensity detected in the $[t_{p_k} - (t_{p_k} - t_{p_{k-1}})/2, t_{p_k}]$ interval.

Applying the peak and nadir detection algorithm to Ca^{2+} signals results in a peak vector $p = (p_1, p_2, ..., p_n)$ indicating the intensities of peaks, a nadir vector $d = (d_1, d_2, ..., d_n)$ showing the intensities of nadirs and a time vector $t_{dp} = (t_{d_1}, t_{p_1}, t_{d_2}, t_{p_2}, ..., t_{d_n}, t_{p_n})$ representing the time points for each element of the p and d vectors where $t_{d_k} < t_{p_k} < t_{d_{k+1}}$. CaSiAn uses the data of detected peaks and nadirs as the input to the other implemented signal analysis methods. Therefore the accuracy of this data is important since it may affect the results of the further analysis steps. Although applying this algorithm to the Ca^{2+} signals results in quite low rate of false positives and true negatives, CaSiAn still provides an interactive interface with which users can manually remove peaks or nadirs that are wrongly detected or add peaks or nadirs that have not been detected by the implemented algorithm. This way, the user has always full control over the signal processing.

S4 Feature Extraction

Extracting descriptors of Ca^{2+} spikes is essential for understanding kinetics of calcium signaling and downstream analyses. CaSiAn measures a set of features that characterize distinguishable signal shapes that helps biologists to have more accurate interpretation of the experimental results (Fig. S4). CaSiAn is able to measure these features for a large amount of Ca^{2+} signals fast and precisely. This opens a new door for Ca^{2+} signal analysis methods, like comparing average intensities, to the wide spectrum of sophisticated data analysis techniques that are more effective and meaningful if they are performed on the signal features instead of large, noisy and redundant signal intensities.

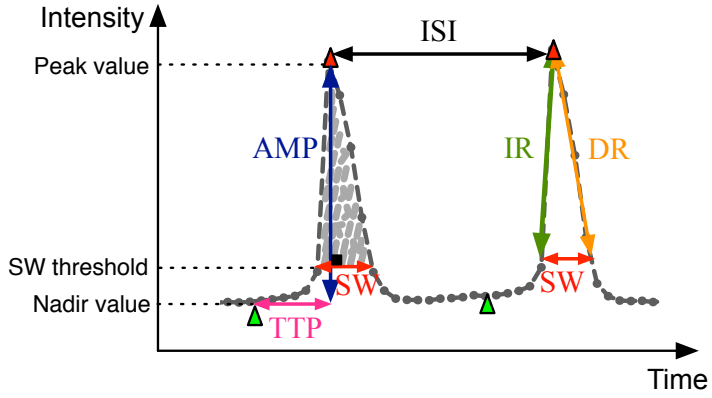

Figure S4. Overview of the Ca^{2+} spike descriptors. CaSiAn quantifies Ca^{2+} spikes by computing the following illustrated features: interspike intervals (ISI), spike amplitude (AMP), spike width (SW), effective area under spike (AUS), increasing rate (IR), decreasing rate (DR), time to peak (TTP), peak intensity, nadir intensity and spike width threshold (TH_{SW}). Red triangles correspond to identified peaks and green triangles to nadirs.

ISI , T_{av} and σ . The interspike interval (ISI) is the time between two Ca^{2+} spikes, i.e. the time difference between two consecutive peaks. For a signal containing n peaks, $\mathit{ISI\text{-}time} = \{(isi_k, t_{isi_k}), k = 1, ..., (n-1)\}$ is a set of paired values where $isi_k = (t_{p_{k+1}} - t_{p_k})$, $t_{isi_k} = t_{p_k}$ and t_{p_k} is the time at which the k-th peak occurs. Modeling and experimental studies have shown that Ca^{2+} signals are made from random sequences of ISIs of unpredictable length. Each ISI has a large stochastic part that leads to a distribution of ISI values [Skupin *et al.*, 2008, Thurley *et al.*, 2011]. CaSiAn plots *isi* values over t_{isi} values for each signal indicating the variability of ISIs over time. CaSiAn also writes the *isi* values of all signals in an output file. This way, the user is able to plot histograms for all *isi* values of a cell population revealing the distribution of spike times in an experiment. Since different cellular pathways may exhibit different ISI distributions they represent a meaningful characteristics for downstream analyses [Skupin *et al.*, 2010].

For each Ca^{2+} signal, the average of ISI values gives the average period (T_{av}) and the variability is expressed by the standard deviation of ISI (σ). Assume a vector of signals $(sg_1, sg_2, ..., sg_l)$ with $(t_{av1}, t_{av2}, ..., t_{avl})$ and $(\sigma_1, \sigma_2, ..., \sigma_l)$, where l is the total number of signals extracted from a cell population. Statistical analysis of ISIs has shown a linear relation between $t_{av\,j}$ and σ_j $(j = 1, .., l)$ where $t_{av\,j}$ and σ_j are typically of similar magnitude indicating the stochastic dynamic of Ca^{2+} signaling [Skupin and Falcke, 2010]. CaSiAn plots the σ_j values versus $t_{av\,j}$ values for a cell population and then fits a linear function $\Lambda = \alpha T_{av} + \beta$ to the $t_{av\,j}$ and σ_j points using linear regression. The period of Ca^{2+} spikes is one information encoding mechanism of Ca^{2+} signals. Therefore the slope α that gives the relation of the mean ISI (T_{av}) and the standard deviation (σ) for a cell population may indicate the signal-to-noise ratio or information content of the Ca^{2+} signals if such a lin-

ear relation describes the data accordingly. Several studies have shown that this slope is pathway specific, robust against cell to cell variability of Ca^{2+} signals and sensitive to the global negative feedback inhibitions in the cellular Ca^{2+} signaling pathway for several cell types [Skupin *et al.*, 2010, Thurley *et al.*, 2014].

Amplitude (AMP). The spike amplitude (AMP_{sp}) is the difference between spike's extreme intensities. While the peak value shows the highest intensity of a spike, the nadir value may not indicate the lowest intensity of a spike (see Figure S5). Our goal is to find the spike base level while considering the possible asymmetric shape of the spike. For this purpose, we define the lowest point of a spike $po_{base} = (t_{base}, I_{base})$ as the intersection point resulting from crossing two lines, the line L_m that connects the two minimum points located on the spike edges and the vertical line $V_p = t_p$ that goes through the peak point of the spike. The equation of the L_m line is identified using nadir point (t_d, d) of the spike and the minimum point $(t_{d'}, d')$ occurring after the spike peak.

Let (t_{p_k}, p_k) be the peak point and (t_{d_k}, d_k) be the nadir point of the k-th spike and $(t_{d_{k+1}}, d_{k+1})$ is the nadir of $(k+1)$-th spike. The minimum point occurring after k-th peak, $po_{d\prime_k} = (t_{d'_k}, d'_k)$, is the solution of the following objective function:

$$O(po_{d\prime_k}) = \min_{t_{p_k} < t \leq t_{d_{k+1}}} \{f(t) - d_k\} \tag{S8}$$

$$\text{subject to: } po_{d\prime_k} \neq \text{local maximum}$$

The function $O(po_{d\prime_k})$ finds the minimum intensity difference between each point located in the $(t_{p_k}, t_{d_{k+1}}]$ window and the intensity of k-th nadir point (see Fig. S5). The constraint of $O_{d\prime_k}$ function indicates that the solution cannot be a local maximum because the local maxima located between two peaks are considered as noise. After detecting the $po_{d\prime_k}$ point, the equation of the L_{m_k} line is determined as $L_{m_k} = a_k t + b_k$, where the slope a_k takes the following value:

$$a_k = \frac{d'_k - d_k}{t_{d'_k} - t_{d_k}}\,. \tag{S9}$$

Therefore the lowest extreme point $po_{base_k} = (t_{base_k}, I_{base_k})$ of the k-th spike results from the crossing of the L_{m_k} line and the vertical line $V_{p_k} = t_{p_k}$ and equals to $(t_{p_k}, a_k t_{p_k} + b_k)$. This determines the amplitude of k-th spike as $AMP_{sp_k} = p_k - I_{base_k}$.

Let $\{AMP_{sp_1}, AMP_{sp_2}, ..., AMP_{sp_n}\}$ be the set of spike amplitudes of a signal. Then the average of spike amplitudes AMP_{sg} identifies the signal amplitude:

$$AMP_{sg} = \frac{1}{n}\sum_{k=1}^{n} AMP_{sp_k}, \tag{S10}$$

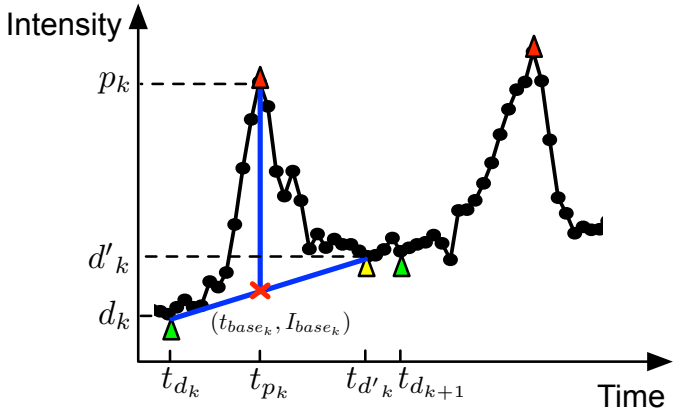

Figure S5. Spike amplitude (AMP). The spike amplitude is equivalent to the difference between the spike peak intensity and the po$_{base}$ intensity. The red triangles denote the peaks and green triangles the nadirs. The yellow triangle is the minimum point detected after the spike peak. The $po_{base} = (t_{base}, I_{base})$ results from the intersection of the vertical line that passes through the spike peak and the line that connects the spike nadir and the minimum point detected after the peak. Note that for this zoom into the example signal no background extraction was performed. The resulting base level trend demonstrates the robustness of the implemented amplitude detection since it is considering local trends and leads to more robust amplitude estimations.

where n is the total number of spikes in the signal.

Spike Width (SW). The width of a Ca^{2+} spike is the duration of the spike when the Ca^{2+} channels are highly activated and the intracellular Ca^{2+} concentration is higher than the base level concentration. CaSiAn identifies the Ca^{2+} spike width (SW_{sp}) as the duration of spike at 20% of the spike amplitude. Let AMP_{sp} be the amplitude, and I_{base} be the base level of a spike, then the spike width threshold TH_{SW} is:

$$TH_{SW} = 0.2\, AMP_{sp} + I_{base}. \tag{S11}$$

The intensity values that are larger than the TH_{SW} value occur in the effective duration of the spike (Fig. S6). In order to measure the width of a spike, we compute the time difference between two points of the spike that have the intensity values equivalent to the spike width threshold. Let $st_{SW} = (t_{st}, st)$ be the point where the effective duration of the spike starts and $en_{SW} = (t_{en}, en)$ be the point where the effective duration of the spike ends. The spike width value is then equal to the difference between t_{st} and t_{en}. The coordinates of the st_{SW} and en_{SW} points are identified from the intersection of $intensity = TH_{SW}$ line and the spike function. But Ca^{2+} signal data are discrete-time functions that may not contain sample points with the TH_{SW} intensity value. Therefore, for finding the width of a spike, we perform upsampling, i.e., constructing new data points by interpolation. For this purpose, we find $A = (t_A, f(t_A))$ and $B = (t_B, f(t_B))$, the two neighbor points on the upward edge, and $C = (t_C, f(t_C))$ and $D = (t_D, f(t_D))$, the two neighbor points on the downward edge of the k-th

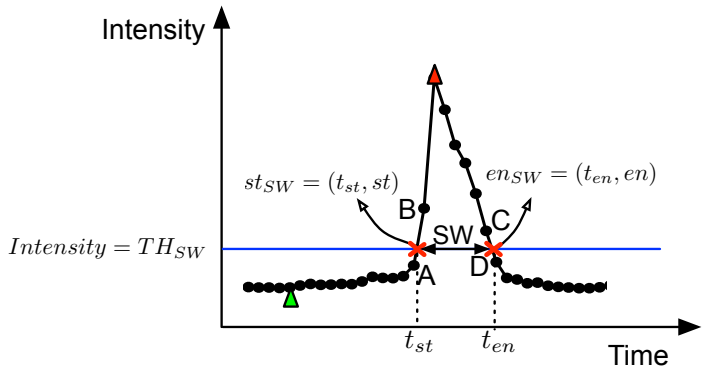

Figure S6. Spike width (SW). The spike width of a Ca^{2+} spike is computed as spike duration at 20% of spike amplitude.

spike, where $t_A < t_B < t_C < t_D$, $f(t_A) \leqslant TH_{SW_k} < f(t_B)$ and $f(t_D) \leqslant TH_{SW_k} < f(t_C)$. The search algorithm explores the $[t_{d_k}, t_{p_k}]$ interval for finding point B as the first sample point with intensity higher than TH_{SW_k}, and explores the $[t_{p_k}, t_{d_{k+1}}]$ interval for finding point D, the first sample point with the intensity lower than the TH_{SW_k} value, where t_{d_k} is the nadir time, t_{p_k} is the peak time of k-th peak and $t_{d_{k+1}}$ is the nadir time of $(k+1)$-th peak. The point A and point C are identified as the prior samples of point B and D, respectively. Then we find the intersection points, st_{SW} and en_{SW}, resulting from crossing the AB and CD lines with the $Intensity = TH_{SW}$ horizontal line, respectively. Finally, the spike width is computed as: $SW = t_{en} - t_{st}$ (Fig. S6).

Let $\{SW_{sp_1}, SW_{sp_2}, ..., SW_{sp_n}\}$ be the set of spike widths of a signal, then the average of spike widths of the signal SW_{sg} specifies the signal spike width:

$$SW_{sg} = \frac{1}{n} \sum_{k=1}^{n} SW_{sp_k}, \tag{S12}$$

where n is the total number of signal spikes.

Time To Peak (TTP). Time to peak of a spike (TTP_{sp}) is the time difference between the peak time and the nadir time of the spike (Fig. S4). The time to peak of a Ca^{2+} signal (TTP_{sg}) is computed by averaging the TTP_{sp} of all spikes in the Ca^{2+} signal.

Root-Mean-Square (RMS) Value. The root-mean-square value, also known as quadratic mean, is a type of average that gives a greater weight to the larger items in the data set. The RMS value of a Ca^{2+} transient may estimate the average of cytosolic Ca^{2+} concentration for the entire Ca^{2+} signal and is rather robust against base level fluctuations. For a Ca^{2+} signal $sg = \{(t_k, f_k), k = 1, .., N\}$, the RMS value is:

$$RMS_{sg} = \sqrt{\frac{\sum_{k=1}^{n} f(k)^2}{N}}, \tag{S13}$$

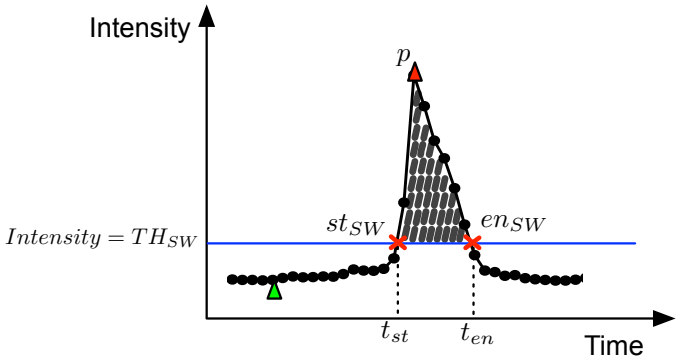

Figure S7. Effective area under a spike (AUS). The effective area under a spike is equivalent to the surface between spike function and the spike width threshold line. CaSiAn estimates AUS using the trapezoidal method.

where N is the total number of sample points in the signal. The RMS can also be used to quantify Ca^{2+} signals in non-spiking conditions like Tcells activation or overstimulation.

Effective Area Under Spike (AUS). The effective area under a spike (AUS_{sp}) is the surface above the horizontal line $Intensity = TH_{SW}$ and the spike function, where TH_{SW} is the threshold of the spike width (Fig. S7). This area can quantify the cellular Ca^{2+} concentration for the effective duration of a spike where Ca^{2+} channels are highly activated [Charlton and Vauquelin, 2010]. The effective area under the spike is a more precise measurement for quantifying the cellular Ca^{2+} concentration compared to the spike amplitude because it also includes information of the spike duration.

We approximate the AUS_{sp} feature by the trapezoidal rule. Let $P(t,I) = \{(t_{st},st),(t_1,f_1),...,(t_m,f_m),(t_{en},en)\}$ be the set of samples that occurs in the effective duration of a spike, where $st_{SW} = (t_{st},st)$ and $en_{SW} = (t_{en},en)$ are the start and end points of the spike duration, respectively and $t_{st} < t_1 < t_m < t_{en}$. The effective area under the spike (AUS_{sp}) is approximated as:

$$AUS_{sp} = \frac{1}{2}\sum_{k=1}^{n}(t_{k+1} - t_k)(I_{k+1} - I_k) \tag{S14}$$

where $n = m+2$ shows the number of points in the P data set.

If $\{AUS_{sp_1}, AUS_{sp_2}, ..., AUS_{sp_n}\}$ is the set of effective spike areas of a Ca^{2+} signal, then the average spike areas AUS_{sg} is computed as:

$$AUS_{sg} = \frac{1}{n}\sum_{k=1}^{n} AUS_{sp_k}, \tag{S15}$$

where n is the total number of signal spikes.

Ca^{2+} Increasing Rate (IR) and Ca^{2+} Decreasing Rate (DR). During a spike, the Ca^{2+} fluxes into the cytoplasm (J_{in}) are counteracted by the fluxes that remove Ca^{2+} from cyto-

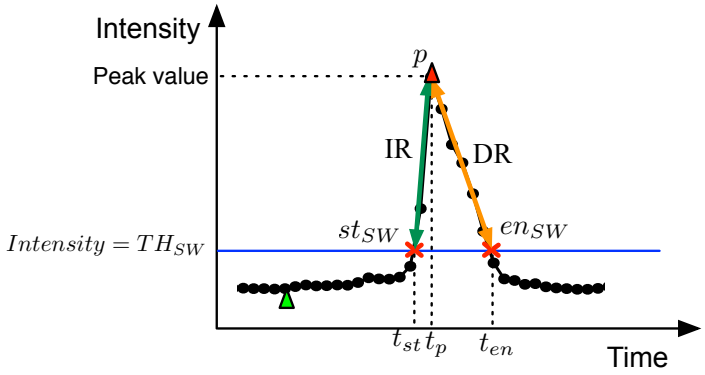

Figure S8. Increasing Rate (IR) and Decreasing Rate (DR). The rate of rising cytosolic Ca^{2+} concentration is equivalent to the slope of the upward edge of a spike (green line). The rate of decreasing cytosolic Ca^{2+} concentration is equivalent to the absolute value of the downward slope (of the orange line).

plasm (J_{out}). The resulting net flux leads to an increasing or decreasing Ca^{2+} concentration in the cytoplasm. Therefore the cellular Ca^{2+} concentration ($[Ca^{2+}]$) at time point $(t+1)$ is equivalent to: $[Ca^{2+}]_{t+1} = [Ca^{2+}]_t + J_{in_{t+1}} - J_{out_{t+1}}$. The upward edge of a Ca^{2+} spike shows the period in which the net Ca^{2+} influx is higher than the net Ca^{2+} efflux resulting in an increasing cellular Ca^{2+} concentration. The downward edge of a Ca^{2+} spike indicates the period where the rate of Ca^{2+} removal is higher than the rate of Ca^{2+} release leading to a dropping cellular Ca^{2+} concentration to the resting level.

CaSiAn estimates the rate of increasing cytosolic Ca^{2+} (IR) by computing the slope of the upward edge of each spike. Analogously, it approximates the decreasing rate (DR) by computing the slope of the downward edge of spike. Let $p = (t_p, p)$ be the peak point, $st_{SW} = (t_{st}, st)$ the start point and $en_{SW} = (t_{en}, en)$ the end point of the effective duration of a spike (Fig. S8). Then the increasing rate IR_{sp} and the decreasing rate DR_{sp} of a Ca^{2+} spike is computed as:

$$IR_{sp} = \frac{p - st}{t_p - t_{st}}, \tag{S16}$$

$$DR_{sp} = -\left(\frac{p - en}{t_p - t_{en}}\right), \tag{S17}$$

where we compute the absolute value for DR_{sp}.

CaSiAn also measures the increasing rate and the decreasing rate of a Ca^{2+} signal by averaging the increasing rates and the decreasing rates of all spikes in the Ca^{2+} signal, respectively.

Other Features. CaSiAn also determines the following further features for each Ca^{2+} signal: mean of intensities, standard deviation of intensities, signal-to-noise ratio, average of the peak values and average of the nadir values.

S5 Quick guide

CaSiAn is implemented in Java to guaranty platform independence and was tested under OS X (10.8.5), Windows (Windows 10) and Linux (Ubuntu 16.04). CaSiAn uses the open source Jfreechart library (http://www.jfree.org/jfreechart/) for diverse plotting routines. Installation of CaSiAn requires Java 8 and is straightforward due to provided installers of the most recent released versions on the project page (http://r3lab.uni.lu/web/casa/). After installation, CaSiAn can be launched and will open a GUI by which the CaSiAn analysis workflow can be controlled. Fig. S9 gives an overview of the CaSiAn workflow that consists of three steps:

1. creating and initializing an experiment workspace, i.e. a container for the Ca^{2+} signal inputs and configuration data (setup),
2. interactively refining the input signals (data curation), and
3. computing the characteristics of Ca^{2+} signals (feature extraction).

Below, we describe the three steps in detail. For a detailed step by step introduction for the most recent version of CaSiAn please also visit the "Getting started" tutorial on the webpage (http://r3lab.uni.lu/web/casa/started.html).

S5.1 Setup

In the Setup step, the user creates an experiment workspace, which is a data structure used to store the input data, experiment configurations, and store the analysis results. The user creates a workspace for an experiment by doing the following steps in the GUI shown in Fig. S10:

1. Browse the directory of signal files (*.xls, *.txt, *.csv, *.dat) of one experiment.
2. Enter a common string among input file names allowing to combine several files that belong to one experiment and ensure unique data handling.
3. Enter a common string among the column header names that contain the intensities of Ca^{2+} signals to be analysed. This allows e.g. to analyse a file containing not only the signals of interest but additional information like individual signals of a radiometric dye.
4. Enter the number of the column that contains the time of the Ca^{2+} signals. If the time column contains the actual acquisition time, the tool will directly use this time and the Time Scaling Factor should be kept as 1. If the time column contains only the frame number of the observed intensities instead of the real acquisition times, the user can enter the corresponding Time Scaling Factor (e.g. the time difference between two consecutive images) in the specified input field and CaSiAn will then compute the

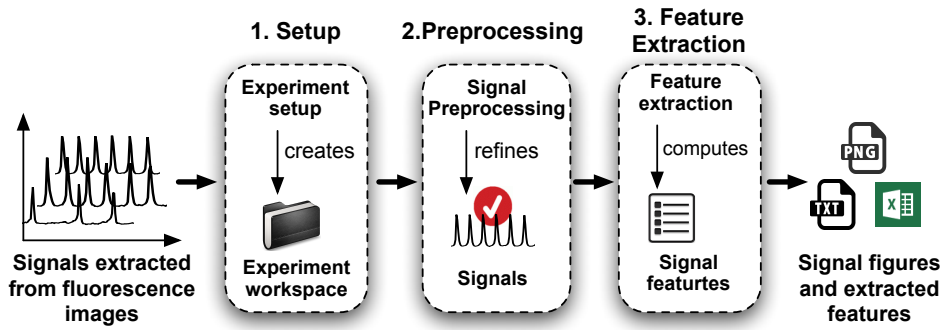

Figure S9. An overview on the CaSiAn workflow. The CaSiAn workflow consists of three steps from loading the data to exporting the quantified signal descriptors described in Section S4.

corresponding time of each sample point by multiplying the frame number with the time difference between two consecutive images.

5. Identify the names of treatments during the imaging, if there is anyone.
6. Load signals in the CaSiAn by clicking on the "open experiment" button.

S5.2 Preprocessing

In the Preprocessing step, the user determines the signal periods to be analyzed, removes background from the signal intensities and can normalize the signal amplitudes for non-ratiometric dye measurements. After the setup step, CaSiAn visualizes the loaded Ca^{2+} signals and the user can go through all signals and edit the signal length individually. In experiments in which cells are stimulated, the Ca^{2+} response often exhibits a transient phase that may be related to the establishment of the steady state regime of IP_3 synthesis and degradation. For the spiking analysis this period should be excluded what can be easily done by specifying the analysis period with the "From" and "To" fields. If there was any perturbation during the measurement, the user can divide signals into sections and analyze the data of each condition separately. For the background removal and signal normalization, the user should select the appropriate curve for estimating the background intensities as described in Section S2 and exemplified in Figure S2. After choosing the proper fitting, the user can subtract the background intensities from the signal intensities by clicking on the "Subtract background" button and also normalize signal intensities by clicking on the "Normalize" button.

S5.3 Feature Extraction

During the Feature Extraction step, CaSiAn finds the peaks and nadirs of Ca^{2+} signals using the peak threshold parameter as discussed in section S3. The user can set the peak threshold parameter either for all signals or for each signal individually. Then CaSiAn visualizes

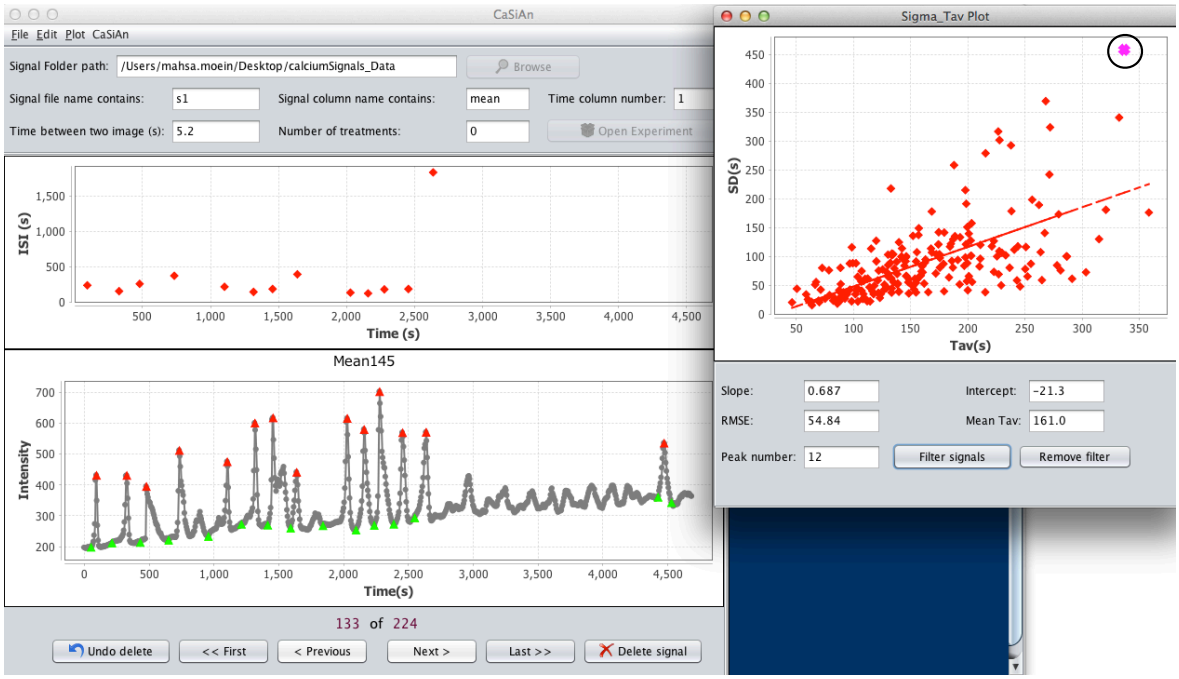

Figure S10. Linear regression between σ and T_{av} is shown in the interactive popup window. In this window, the data can be filtered by the number of spikes and clicking on a (σ, T_{av}) tuple (shown by circle) will display the corresponding spike train in the main window.

the result of the peak and nadir detection process and the user is able to examine them by scrolling through the signals. If any peak or nadir point is not detected or is detected wrongly, the user can easily right click on it and add it to the list of peaks or nadirs or remove it from the list. After identification of peaks and nadirs in the signals, CaSiAn computes all other signal characteristics as described in Section S4. In particular, CaSiAn calculates T_{av} and σ for all signals which can then be visualized in an interactive popup window depicting the σ - T_{av} relation as shown in Fig. S10. In this window, the considered signals can be filtered by the number of minimal ISI a signal must have and clicking on any (T_{av},σ) tuple will load the corresponding signal in the signal viewer panel of the main window. Finally, the user can access all computed features in the form of a text or excel file by clicking on the "Export Data and Figures" button.

S6 Materials and Methods

S6.1 Ca^{2+} Imaging in C8-D1A cells

Cells were grown in poly-L-lysine-coated cover-slips for three days in DMEM medium (Thermofisher, A14430-01) containing 25 mM glucose, 4 mM glutamine supplemented with 10% fetal bovine serum and 1% penicillin streptomycin until ˙ 80 % confluency. Then cells

were washed with phosphate buffered saline (PBS) and new phenol red free medium containing 25 mM glucose, 4 mM glutamine, supplemented with 10% fetal bovine serum and 1% penicillin streptomycin were added to the cells. Then cells were loaded with 250 μl of Fluo-4 Direct from Thermofisher for 30 min in the incubator and then immediately transferred to an imaging chamber at 37°C. Cells were imaged on Nikon Ti Eclipse inverted microscope using excitation at 490 to 510 nm (ET500/20x filter from Chroma) with a sample rate of 0.33 s^{-1}. The exposure time was set to 80 ms. During imaging cells are treated to 10 μM ATP (Sigma-Aldrich, A1852-1VL) for 27 minutes and 80 μM ATP for 37 minutes as indicated in Fig. S1 by red and blue bars, respectively.

After acquisition of images for three independent experiments, Ca^{2+} signals were extracted using ImageJ (version 1.48) and exported as excel files. These files were loaded into the CaSiAn workflow and analyzed as described in the main text and shown in Fig. S1. The additional results are shown in Fig. S11.

S6.2 Zebrafish Calcium Imaging

To demonstrate the broad application spectrum of CaSiAn, we also analyzed data obtained from an *in vivo* study on drug induced epileptic seizure genesis in zebrafish.

Animals: Adult zebrafish were kept at 26-27°C in a 14 hour light/10 hour dark cycle. The Tg(actb2:GCaMP6f) line was used for all experiments. This line expresses GCaMP6f under the zebrafish beta-actin promoter and was generated by injecting an actb2:GCaMP6f construct flanked by tol2 sites into one-cell stage embryos together with tol2-transposase. To obtain a stable transgenic line, injected embryos were raised, adult fish were screened for transgenic offspring, and transgenic embryos were raised to adulthood.

For the experiments, embryos were obtained by natural spawning and fertilized eggs were raised at 28.5°C in E3 solution (5mM NaCl, 0.17mM KCl, 0.33mM $CaCl_2.2H_2O$, 0.33mM $MgSO_4.6H_2O$). At 1 day post-fertilization (dpf), 1-phenyl 2-thiourea (PTU; Sigma-Aldrich) 0.003% in E3 was added to the embryos to suppress pigmentation. Exchange of the medium was performed daily to ensure the viability of the embryos/larvae, and larvae were used at 5 dpf for the experiments.

Chemicals: The chemicals used in this study were Picrotoxin and DMSO (both from Sigma-Aldrich). Picrotoxin was dissolved in DMSO and diluted in E3 medium to a final concentration of 1mM containing 1% v/v of DMSO. DMSO 1% v/v in E3 was used as a vehicle control.

Confocal imaging: 5dpf Tg(actb2:GCaMP6f) zebrafish transgenic larvae were mounted in-

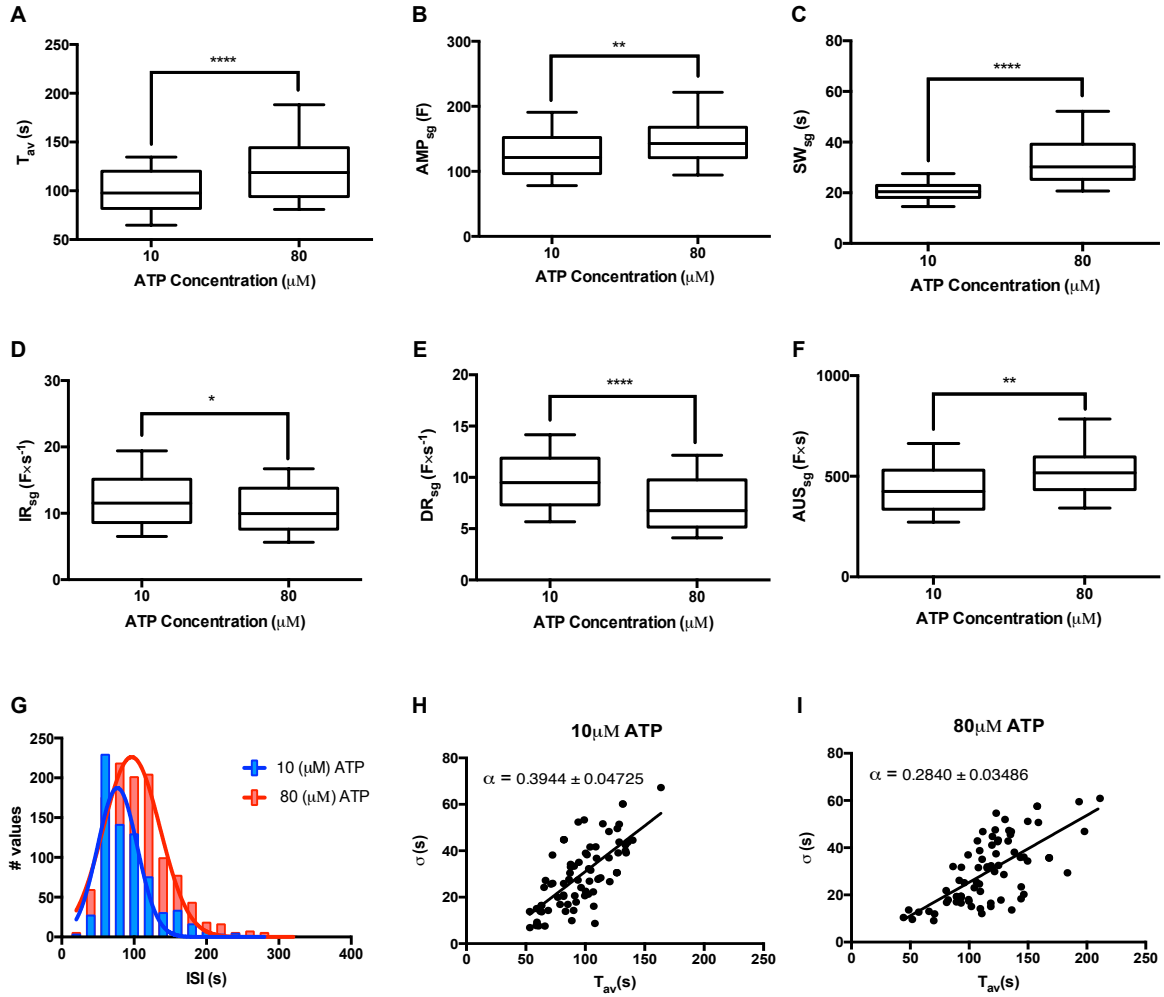

Figure S11. Statistical analysis of astrocytic Ca^{2+} signal features for 2 different stimulation periods of 10 μM and 80 μM ATP as described in the main text. All shown features exhibit significant differences for the different stimulation strengths tested by unpaired t-test in Prism (version 6, GraphPad Software) with significance levels $p \leq 0.05 = {}^{*}$, $p \leq 0.01 = {}^{**}$, and $p \leq 0.001 = {}^{****}$.

	Hind brain	Right OT	Left OT
AUS_{sp} vs. ISI	0.856	0.6794	0.4228
Following ISI vs. ISI	0.8275	0.6515	0.6299

Table S1. Correlation between some CaSiAn features for the 3 different brain regions considered.

dividually in glass bottom petri dishes (MatTek) with 1.3% low melting point agarose (PeqGold) and incubated with 1mM picrotoxin or with vehicle control. A time-lapse imaging was started 5 minutes after incubation with the drug or vehicle at room temperature using a laser scanning confocal microscope (LSM780, Zeiss). The following imaging parameters were used: objective Plan-Apochromat 20x/0.8, 488 nm laser illumination, pixel dwell time 2.55 μs, pixel size 1.661 μm, format 256 x 256 pixels, 16-bit depth image, 5 μm optical sectioning, focal plane at a 50-65 μm deepness from the dorsal brain skin, and image acquisition at 5 frames per second. After imaging, the temperature of the medium in the plates was monitored and ranged between 26-27.5°C.

Image Analysis: The mean fluorescence intensity of regions of interests (ROI) was calculated using ImageJ (version 1.51j). Briefly, a reference stack was generated for each time-lapse image (by averaging image frames) and ROI were manually outlined from three anatomically distinct brain regions: left optic tectum (OT), right OT and hindbrain (Fig. S12). Afterwards, the ROI were applied to the original time-lapse and the mean fluorescence intensity for each frame was exported to an *xls file.

The file was then loaded into the CaSiAn software for the analysis of Ca^{2+} signals of 45 minutes time-lapse recording. A polynomial regression curve was applied for background removal and data normalization. Afterwards, peaks and nadirs were determined by the software using the peak threshold parameter, followed by manual curation of false positive or negative peaks. Finally, Ca^{2+} signal features were extracted and exported for analysis by GraphPad. The time course data and corresponding analysis is visualized in Fig. S12 and correlation values are given in Tab. S1.

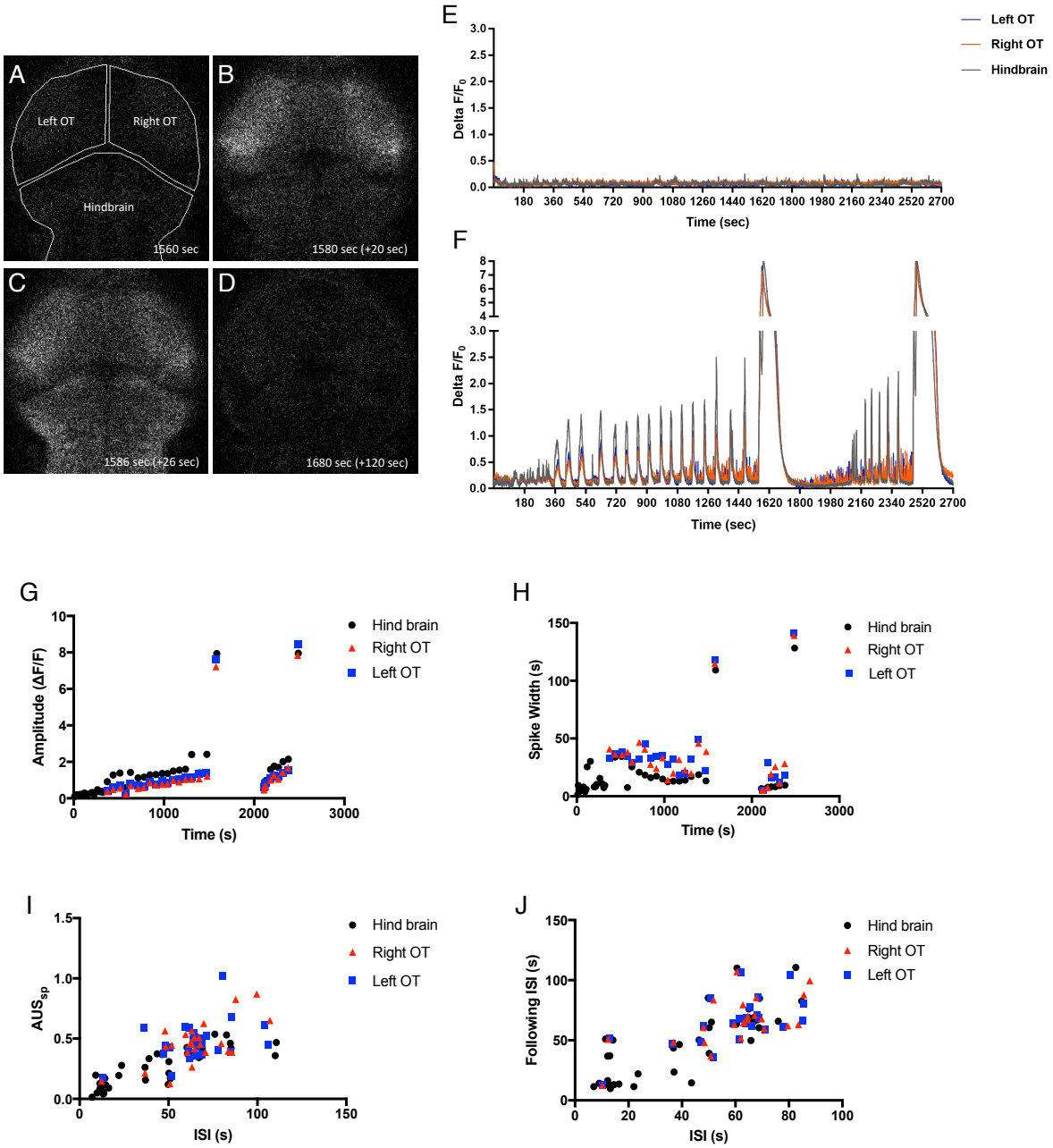

Figure S12. Analysis of seizure genesis in zebrafish. A-D: Definition of the brain region and snapshots of signal intensities for the indicated time points. E, F: Extracted time course data for control (E) and drug induced activity with picrotoxin (F). G: The dynamics of spike amplitudes for all 3 brain regions show an smooth increase up to a big jump that corresponds to the large global activity peak. H: The temporal behaviour of the spike width exhibits an intermediate decrease before the pronounced global activity spike further indicating the increasing synchronization. I: Dependence between the area under a spike (AUS) and the ISI. J: The correlation between successive ISI further demonstrates the drug induced synchonization dynamics.

Bibliography

[Balkenius *et al.*, 2015] Balkenius,A., Johansson,A.J. and Balkenius,C. (2015) Comparing analysis methods in functional calcium imaging of the insect brain. *PloS One,* 10 (6), e0129614.

[Charlton and Vauquelin, 2010] Charlton,S.J. and Vauquelin,G. (2010) Elusive equilibrium: the challenge of interpreting receptor pharmacology using calcium assays. *British Journal of Pharmacology,* 161 (6), 1250–1265.

[Diaspro *et al.*, 2006] Diaspro,A., Chirico,G., Usai,C., Ramoino,P. and Dobrucki,J. (2006) Photobleaching. In *Handbook of biological confocal microscopy*. Springer pp. 690–702.

[Janicek *et al.*, 2013] Janicek,R., Hotka,M., Zahradníková Jr,A., Zahradníková,A. and Zahradník,I. (2013) Quantitative analysis of calcium spikes in noisy fluorescent background. *PloS One,* 8 (5), e64394.

[Mikhailyuk and Razzhivin, 2003] Mikhailyuk,I. and Razzhivin,A. (2003) Background subtraction in experimental data arrays illustrated by the example of raman spectra and fluorescent gel electrophoresis patterns. *Instruments and Experimental Techniques,* 46 (6), 765–769.

[Skupin and Falcke, 2010] Skupin,A. and Falcke,M. (2010) Statistical analysis of calcium oscillations. *The European Physical Journal Special Topics,* 187 (1), 231–240.

[Skupin *et al.*, 2010] Skupin,A., Kettenmann,H. and Falcke,M. (2010) Calcium signals driven by single channel noise. *PLoS Comput Biol,* 6 (8), e1000870.

[Skupin *et al.*, 2008] Skupin,A., Kettenmann,H., Winkler,U., Wartenberg,M., Sauer,H., Tovey,S.C., Taylor,C.W. and Falcke,M. (2008) How does intracellular Ca^{2+} oscillate: by chance or by the clock? *Biophysical Journal,* 94 (6), 2404–2411.

[Thurley *et al.*, 2011] Thurley,K., Smith,I.F., Tovey,S.C., Taylor,C.W., Parker,I. and Falcke,M. (2011) Timescales of Ip_3-evoked Ca^2+ spikes emerge from Ca^2+ puffs only at the cellular level. *Biophysical Journal,* 101 (11), 2638–2644.

[Thurley *et al.*, 2014] Thurley,K., Tovey,S.C., Moenke,G., Prince,V.L., Meena,A., Thomas,A.P., Skupin,A., Taylor,C.W. and Falcke,M. (2014) Reliable encoding of stimulus intensities within random sequences of intracellular Ca^{2+} spikes. *Science Signaling,* 7 (331), ra59.

[Waters, 2009] Waters,J.C. (2009) Accuracy and precision in quantitative fluorescence microscopy. *The Journal of Cell Biology,* 185 (7), 1135–1148.